(Preprint) AAS 19-801

SUN-AVOIDANCE SLEW PLANNING ALGORITHM WITH POINTING AND ACTUATOR CONSTRAINTS

Mohammad Ayoubi*and Junette Hsin†

This paper presents a geometric approach for a sun (or any bright object) avoidance slew maneuver with pointing and actuator constraints. We assume spacecraft has a single light-sensitive payload with control-torque and reaction wheels' angular momentum constraints. Furthermore, we assume the initial and final attitudes, instrument boresight vector, and sun vector are known. Then we use Pontryagin's minimum principle (PMP) and derive the desired or target-frame quaternions, angular velocity and acceleration. In the end, a Monte Carlo simulation is performed to show the viability of the proposed algorithm with control-torque and angular momentum constraints.

INTRODUCTION

Large-angle slew maneuvers are required during any Earth-pointing or interplanetary missions. In many space missions, and for safety consideration, a sensitive payload such as imaging camera or telescope needs to be retargeted while avoiding the sun vector or other bright objects in the sky.

The attitude reorientation problem in the presence of attitude constrained zones has been studied in the last three decades. McInnes[1] addressed this problem via an artificial potential function. He proposed an entirely analytical guidance law which was suitable for onboard implementation. However, he used Euler angles, which are singular for large slew angles.

A geometric approach was proposed by Spindle,[2] Hablani,[3] and Biggs and Colley[4] where a feasible attitude maneuver, or a guidance law, is precomputed based on the attitude-avoidance-zone constraints. Another approach for addressing this problem used randomized algorithms.[5] However, depending on the number of constraints and initial and final attitudes, this approach can be computationally expensive and not suitable for onboard implementation.

Another approach for solving the time optimal reorientation maneuver subject to boundaries and path constraints was proposed by Spiller et al.[6] They used the particle swarm optimization (PSO) technique to find a sub-optimal solution with keep-out constraints. Another approach casted the problem as a convex optimization problem and used semi-definite programming (SDP) or quadratically constrained quadratic programming (QCQP) in its solution (see for instance Kim and Mesbahi,[7] Kim et al.,[8] Sun and Dai,[9] and Lee and Mesbahi[10]). Recently, Ramos and Schaub[11] proposed

*Associate Professor, Department of Mechanical Engineering, Santa Clara University, 500 El Camino Real, Santa Clara, CA 95053 U.S.A. AIAA senior member, AAS senior member.

†Engineer, Dynamics and Control Analysis Group, Maxar Space Solutions (formerly Space Systems/Loral), 3825 Fabian Way, Palo Alto, CA 94303 U.S.A.

a method based on the Lyapunov stability theorem and logarithmic barrier potential function to derive a steering law for attitude control of a spacecraft subject to conically constrained inclusion and exclusion regions. They also considered the control-torque constraint in their algorithm.

In this paper, we present a novel geometric approach for large-angle slew planning with pointing and actuator constraints. We assume that the spacecraft has a single light-sensitive payload with control-torque and reaction wheels' angular momentum constraints. Furthermore, we assume that the initial and final attitudes, instrument boresight vector, and sun vector are known. Then, we derive the desired or target-frame quaternions, angular velocities, and angular accelerations based on the Pontryagin's minimum principle (PMP) for the proposed maneuver.

The proposed algorithm in this paper is intuitive, deterministic, easy to implement, and includes the control-torque and reaction wheels' angular momentum constraints. The main drawback of the proposed algorithm is its limitation for a single sensitive-payload. A Monte Carlo simulation is performed to show the viability of the proposed algorithm with control-torque and angular momentum constraints.

STEERING LAWS

Calculate the threshold triangle as ϕ_t,

$$\phi_t = \dot{\omega}_{max}/\ddot{\omega}_{max}; \tag{1}$$

Using the conditions, $\dot{\phi}(t_1) = \dot{\phi}_{max}$, $\dot{\phi}(t_f) = \dot{\phi}_f$, $\phi(t_f) = \phi_f$, if $\phi > \phi_t$, then we can determine switching times t_1, t_2, and final time t_f as:

$$t_1 = t_0 + \frac{\dot{\phi}_{max} - \dot{\phi}_0}{\ddot{\phi}_{max}}, \tag{2}$$

$$\begin{aligned} t_2 =& t_1 + \frac{1}{\dot{\phi}_{max}}\Big[\phi_f - \dot{\phi}_0(t_1 - t_0) - \frac{1}{2}\ddot{\phi}_{max}(t_1 - t_0)^2 \\ & - \frac{\dot{\phi}_{max}(\dot{\phi}_{max} - \dot{\phi}_f)}{\ddot{\phi}_{max}} + \frac{(\dot{\phi}_{max} - \dot{\phi}_f)^2}{2\ddot{\phi}_{max}}\Big], \end{aligned} \tag{3}$$

and

$$t_f = t_1 + \frac{1}{\dot{\phi}_{max}}\Big[\phi_f - \dot{\phi}_0(t_1 - t_0) - \frac{1}{2}\ddot{\phi}_{max}(t_1 - t_0)^2 + \frac{(\dot{\phi}_{max} - \dot{\phi}_f)^2}{2\ddot{\phi}_{max}}\Big]. \tag{4}$$

If $\phi \leq \phi_t$, then the switching times are determined by:

$$t_f = \sqrt{\frac{\dot{\phi}_{max}^2}{\ddot{\phi}_{max}}} \tag{5}$$

$$t_2 = \frac{t_f}{2} \tag{6}$$

$$t_1 = t_2 \tag{7}$$

NUMERICAL SIMULATION

The proposed algorithm was examined by running cases in which the initial, final, and sun position vectors were randomized. Consider a spacecraft as a rigid body with one sensitive instrument. The orientation of the boresight of the instrument to the spacecraft body axes, the current and final (desired) positions with respect to the inertial frame, and the location of the sun vector are known. Only one exclusion zone around a bright object (the sun) is considered. The initial and final positions are outside of the exclusion zone.

Algorithm 1 Slew Maneuver Check

```
Find eigenaxis, ${}_{\mathcal{N}}e$ of slew plane
    Compute cross product of $P_i$ and $P_f$ unit vectors
Compute angle between sun vector and slew plane angle $\alpha$
if $|\alpha| < \epsilon_p$ then
    Execute sun-avoidance slew:
        Find $\vec{S}_{||}$
        Compute $\phi_1$, $\phi_2$, $\phi_3$
else
    Slew directly from $P_i$ to $P_f$
end if
```

Algorithm 2 Steering Profiles

```
Compute $\phi_t$
Compute switching times $t_1$, $t_2$, $t_f$ for $\phi_1$, $\phi_2$, and $\phi_3$:
if $\phi > \phi_t$ then
    Use equations 2 through 4
else
    Use equations 7 through 5
end if
for $t_0 < t < t_1$ do
    Calculate inertial-to-desired rotation ${}^{D}R^{N}$
    From ${}^{D}R^{N}$, calculate ${}_{\mathcal{B}}\dot{\omega}^{D}$
        Solve for control torque $u$ with equation 9
        Propagate $\omega$ and $q$ by solving equations 9 and 10
end for
Repeat above lines for $t_1 < t < t_2$ and $t_2 < t < t_f$
```

The results show that the angular velocity and acceleration never exceed the velocity and acceleration constraints for any axis. There is no noise modeled in the actuator system, as the purpose of this simulation was to validate the slewing maneuvers described by the algorithm.

The attitude and rates were computed within each switching time interval for a constant control torque. The desired acceleration in the body frame, ${}_{\mathcal{G}}\ddot{\phi}_{max}$ rotates around the eigenaxis ${}_{\mathcal{N}}e$ or sun vector ${}_{\mathcal{N}}S$, which are both fixed in the inertial frame. To find ${}_{\mathcal{G}}\ddot{\phi}_{max}$, the rotation from the inertial to (desired) body frame needed to be calculated, which is possible from:

$$ {}^{D}R^{N} = \left[(cos\phi)I_{3x3} + (1 - cos\phi)\hat{e}\hat{e}^{T} - (sin\alpha)E^{x}\right] \tag{8} $$

With the desired direction of acceleration in the body frame known, the necessary control torque can be solved for using Euler's equations for rigid body dynamics:

$$J \cdot_{\mathcal{G}} \dot{\omega}^D = u - {}_{\mathcal{G}}\omega^G \times J \cdot_{\mathcal{G}} \omega^G \tag{9}$$

where ${}_{\mathcal{G}}\omega^G$ is the current angular velocity in the body frame. The spacecraft was assumed to be a simple rigid body for algorithm demonstration purposes. Once u was solved, the propagation of ω and q was performed by discretely solving equation 9 and the kinematical equations of motion, equation 10, with a simulation rate of 100 Hz.

$$\dot{q} = \frac{1}{2}\Omega q, \tag{10}$$

where Ω is

$$\Omega = \begin{bmatrix} 0 & \omega_3 & -\omega_2 & \omega_1 \\ -\omega_3 & 0 & -\omega_1 & \omega_2 \\ \omega_2 & -\omega_1 & 0 & \omega_3 \\ -\omega_1 & \omega_2 & -\omega_3 & 0 \end{bmatrix} \tag{11}$$

For the interval from t_1 to t_2, the acceleration due to applied control torque was $\ddot{\phi}_{max}$. For the interval from t_1 to t_2, the applied control torque of 0. For t_2 to t_f, the acceleration was $-\ddot{\phi}_{max}$ so that the spacecraft could satisfy the boundary condition for velocity at t_f.

Two cases are shown here - one in which the sun angle is greater than 0 from the slew plane. The other case is one in which the sun vector lies directly on the slew plane, so that $\phi_2 = 180$ degrees.

Case I: $\alpha > 0$

The parameters for a test case in which the sun vector did not lie directly on the slew plane are shown in Table 1. The calculated slew angles are shown in Table 2.

The constraints for maximum angular velocity and acceleration were chosen to demonstrate that the angular velocity and acceleration profiles would follow the switching times if-else statements, should the ϕ exceed the angle threshold ϕ_t. The spacecraft slews from the initial to the target position during the maneuvers, and P_1 and P_2 are connected via a rotation around the sun vector. This is found to be true no matter the sun vector's position relative to the slew plane.

Table 1. Initial, Final, and Sun Positions in Inertial Frame and Constraints (Sample Inputs)

Unit Vector	Comp
P_i	[-0.50, 0.57, 0.65]
P_f	[0.76, -0.48, -0.44]
S	[0.30, -0.50, -0.81]
Parameter	**Constraint**
$\ddot{\phi}_{max}$	1 rad/s^2
$\dot{\phi}_{max}$	1 rad/s

Table 2. Slew Angles ϕ_1, ϕ_2, and ϕ_3

ϕ	deg
1	32.08
2	102.56
3	17.76

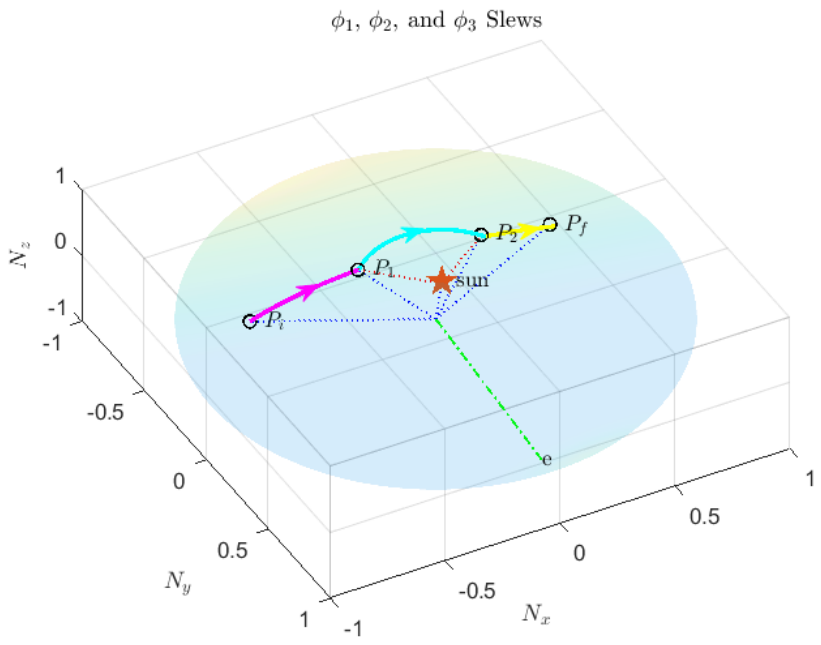

Figure 1. Attitude Profile of the Entire Slew.

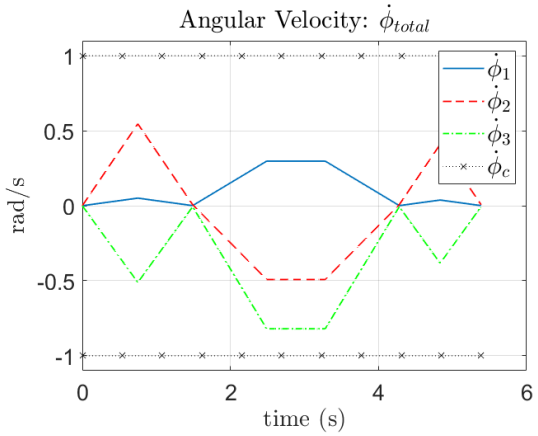

Figure 2. Angular Velocity when $\alpha > 0$.

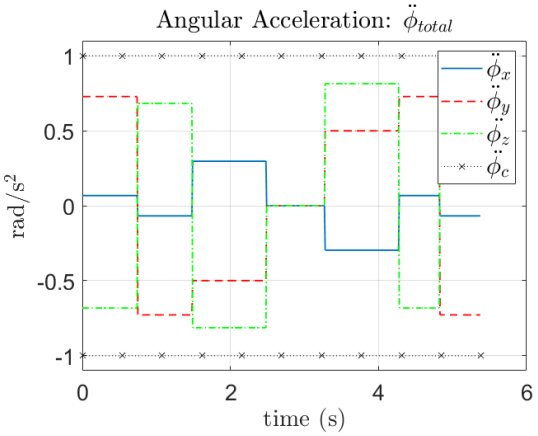

Figure 3. Angular Acceleration when $\alpha > 0$.

Only the angular velocity and acceleration plots have constraints. In real life, the spacecraft's reaction wheels' ability to impart angular momentum is translated to a constraint in angular velocity, and the thrusters ability to impose torque translates to a constraint in angular acceleration. Therefore, there is no torque constraint plotted.

Due to the high velocity and acceleration constraints, there is no coasting period for the ϕ_1 and ϕ_3 portions of the slew. However, there is a period of 0 angular acceleration constant angular velocity

for ϕ_2, which is reflected in the Figures 2 and 3. The attitude and torque profiles are shown in Figures 4 and 5.

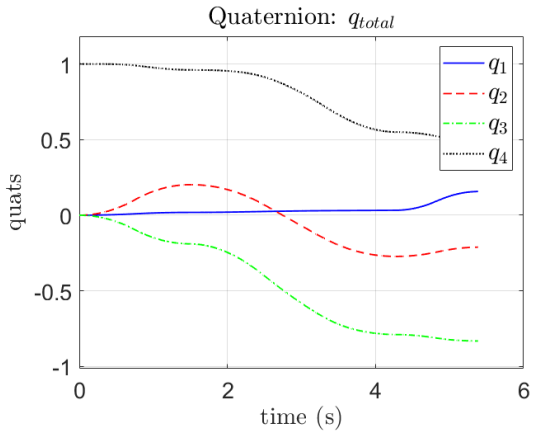

Figure 4. Quaternions when $\alpha > 0$.

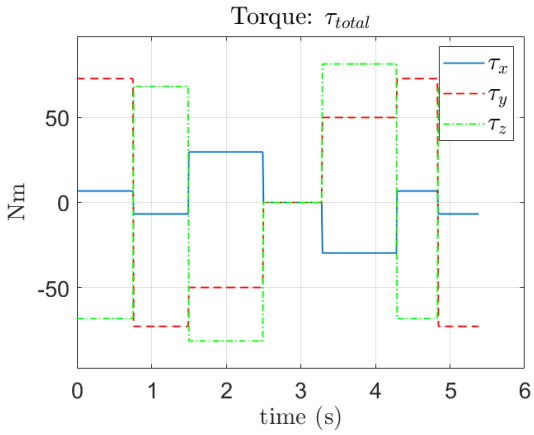

Figure 5. Torque when $\alpha > 0$.

Case II: $\alpha = 0$

For the case in which the sun vector lies directly on the slew plane, ϕ_2 = 180 degrees. The initial, final, and sun positions in the inertial frame and the constraints are in Table 3.

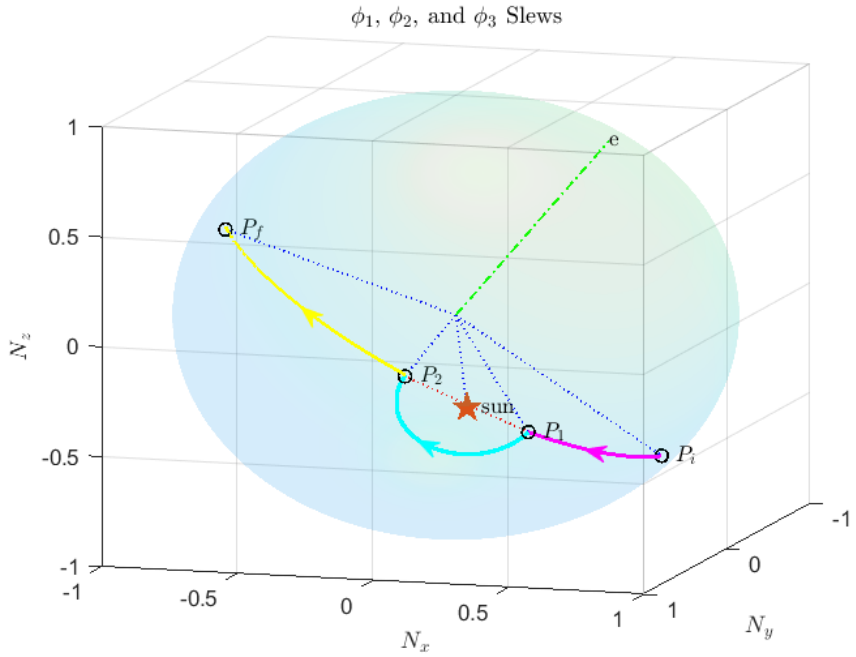

Figure 6. Attitude Profile of the Entire Slew when $\alpha = 0$.

The previous case, in which $\alpha > 0$, had acceleration and velocity constraints of 1 rad/s^2 and 1 rad/s respectively, to demonstrate the if-else statements for switching times in case $\phi > \phi_t$. For this example, much more realistic constraints were imposed to reflect how the acceleration and velocity profiles would look like in real life.

Table 3. Initial, Final, and Sun Positions in Inertial Frame and Constraints (inputs)

Unit Vector	Comp
P_i	[0.65, -0.35, -0.67]
P_f	[-0.93, -0.25, 0.28]
S	[-0.20, -0.78, -0.59]
Parameter	**Constraint**
$\ddot{\phi}_{max}$	0.02 rad/s^2
$\dot{\phi}_{max}$	0.01 rad/s

Table 4. Slew Angles ϕ_1, ϕ_2, and ϕ_3

ϕ	deg
1	41.82
2	180.00
3	62.45

With smaller constraints, the simulation takes much longer to complete the slew maneuvers. Figures 7 and 10 show that the torque and acceleration applied are very short compared to the duration of the entire maneuver, in contrast to Figures 3 and 5. The spacecraft spends the majority of the time coasting at constant angular velocity, as seen in Figure 8. Though the initial and final points are further apart in the gyrostat unit sphere to begin with, the simulation takes an order of magnitude longer to complete at almost 500 seconds for $\alpha = 0$, as opposed to almost 5.5 seconds for $\alpha > 0$. The case shown here is much more realistic example that reflects real-world conditions.

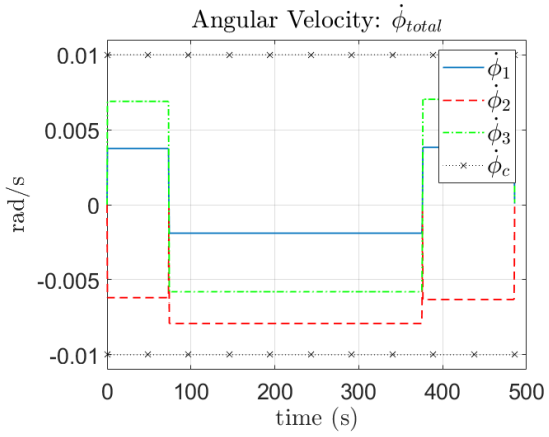

Figure 7. Angular Velocity when $\alpha = 0$.

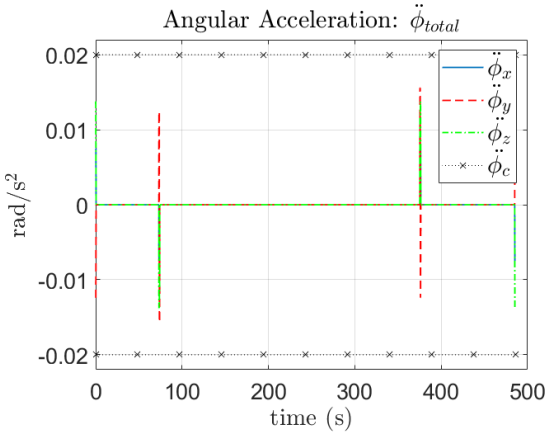

Figure 8. Angular Acceleration when $\alpha = 0$.

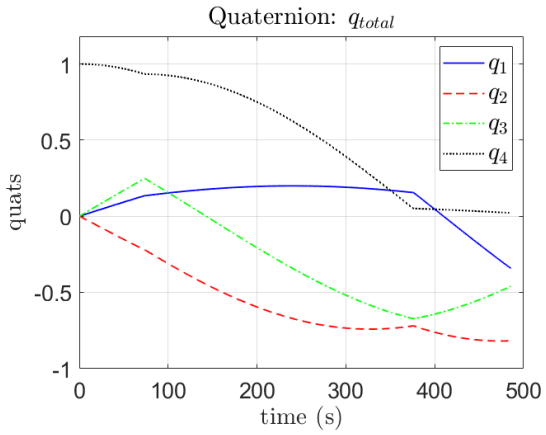

Figure 9. Quaternions when $\alpha = 0$.

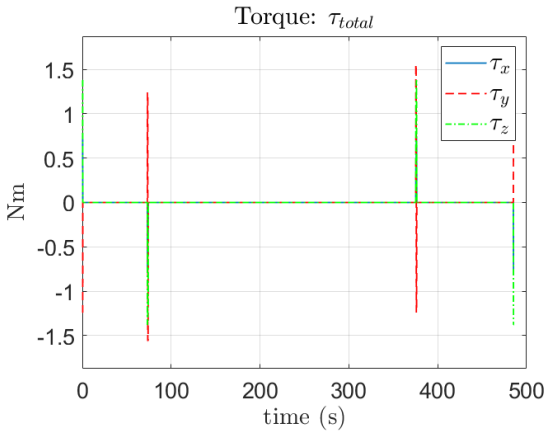

Figure 10. Applied Torque when $\alpha = 0$.

CONCLUSION

A new geometric approach for large-angle slew planning with pointing and actuator constraints is presented. The spacecraft has a single light-sensitive payload with control-torque and reaction wheels' angular momentum constraints. Furthermore, we assume that the initial and final attitudes, instrument line-of-sight vector, and sun vector are known. Then the desired or target-frame quaternions, angular velocities, and angular accelerations are derived based on the PMP. The proposed algorithm is intuitive, deterministic, and easy to implement. The main drawback of the proposed algorithm is its limitation for a single sensitive-payload. The feasibility of the proposed algorithm is demonstrated for two arbitrary cases and it has been investigated via extensive numerical simulations.

ACKNOWLEDGMENT

The research of the authors has been supported by Maxar Space Solutions (Formerly Space Systems / Loral). The second author would like to acknowledge Luke DeGalan for his useful comments.

NOTATION

$\mathcal{G}$-frame	gyrostat body-fixed frame
${}^{\mathcal{N}}H^{\mathcal{G}/\mathcal{G}*}$	the total angular momentum of the gyrostat with respect to its center of mass
$I^{\mathcal{G}/\mathcal{G}^*}$	the mass-moment-of-inertia of the gyrostat
$I^{w/w*}$	the mass-moment-of-inertia of reaction wheels with respect to their center of masses
M_{max}	the maximum available torque along the eigenaxis
$\mathcal{N}$-frame	the Newtonian frame
${}_{\mathcal{G}}\hat{P}$	unit vector along the bore sight of payload in the $\mathcal{G}$-frame
${}_{\mathcal{N}}\hat{P}_i$	unit vector of the initial point in the $\mathcal{N}$-frame
${}_{\mathcal{N}}\hat{P}_f$	unit vector of the final point in the $\mathcal{N}$-frame
${}^{\mathcal{N}}q^{\mathcal{T}}$	quaternion of the $\mathcal{T}$-frame in the $\mathcal{N}$-frame
${}_{\mathcal{N}}\hat{S}$	unit vector of the sun vector in the $\mathcal{N}$-frame
$\mathcal{T}$-frame	the target frame
ϵ_p	Payload half-cone angle
${}^{\mathcal{N}}\alpha^{\mathcal{T}}$	angular acceleration of the $\mathcal{T}$-frame in the $\mathcal{N}$-frame
${}^{\mathcal{N}}\omega^{\mathcal{T}}$	angular velocity of the $\mathcal{T}$-frame in the $\mathcal{N}$-frame

REFERENCES

[1] C. R. McInnes, "Large angle slew maneuvers with autonomous sun vector avoidance," *Journal of Guidance Control Dynamics*, Vol. 17, 06 1994, pp. 875–877, 10.2514/3.21283.

[2] K. Spindler, "New Methods in On-Board Attitude Control (AAS 98-308)," Vol. 100, 01 1998.

[3] H. B. Hablani, "Attitude commands avoiding bright objects and maintaining communication with ground station," *Advances in the Astronautical Sciences*, 1998, 10.2514/2.4469.

[4] J. D. Biggs and L. Colley, "Geometric Attitude Motion Planning for Spacecraft with Pointing and Actuator Constraints," *Journal of Guidance, Control, and Dynamics*, 2016, 10.2514/1.G001514.

[5] E. Frazzoli, M. A. Dahleh, E. Feron, R. P. Kornfeld, and R. P. Kornfeld, "A Randomized Attitude Slew Planning Algorithm for Autonomous Spacecraft," *In AIAA Guidance, Navigation, and Control Conference*, 2001.

[6] D. Spiller, L. Ansalone, and F. Curti, "Particle Swarm Optimization for Time-Optimal Spacecraft Reorientation with Keep-Out Cones," *Journal of Guidance, Control, and Dynamics*, 2016, 10.2514/1.G001228.

[7] Y. Kim and M. Mesbahi, "Quadratically constrained attitude control via semidefinite programming," *IEEE Transactions on Automatic Control*, 2004, 10.1109/TAC.2004.825959.

[8] Y. Kim, M. Mesbahi, G. Singh, and F. Y. Hadaegh, "On the convex parameterization of constrained spacecraft reorientation," *IEEE Transactions on Aerospace and Electronic Systems*, 2010, 10.1109/TAES.2010.5545176.

[9] C. Sun and R. Dai, "Spacecraft Attitude Control under Constrained Zones via Quadratically Constrained Quadratic Programming," 2015, 10.2514/6.2015-2010.

[10] U. Lee and M. Mesbahi, "Quaternion based optimal spacecraft reorientation under complex attitude constrained zones," *Advances in the Astronautical Sciences*, 2014.

[11] M. Diaz Ramos and H. Schaub, "Kinematic Steering Law for Conically Constrained Torque-Limited Spacecraft Attitude Control," *Journal of Guidance, Control, and Dynamics*, Vol. 41, jul 2018, pp. 1990–2001, 10.2514/1.G002873.